Morphological detection and feature-based classification of cracked regions in ferrites

M. Nieniewski[1], L. Chmielewski[2], A. Jóźwik[3], M. Skłodowski[2]

[1]*IFTR, PAS* and *Electrotechnical Institute, Warsaw;* [2]*IFTR, PAS* and *AIP, PL* [3]*IBBE, PAS*
e-mail: mnieniew@ippt.gov.pl, lchmiel@ippt.gov.pl, adamj@ibib.waw.pl, msklod@ippt.gov.pl

Abstract Automatic quality inspection of ferrite products is difficult as their surfaces are dark and in many cases covered with traces of grinding. A two-stage vision system for detection and measurement of crack regions was devised. In the first stage the regions with strong evidence for cracks are found using a morphological detector of irregular brightness changes with subsequent morphological reconstruction. In the second stage the feature-based k-Nearest Neighbors classifier analyzes the pixels indicated in the first stage. The classifier is optimized by using procedures of reclassification and replacement carried out on the reference set of pattern pixels to achieve a low error rate and a maximum speed of computation.

Keywords: morphological defect detection, surface defects, morphological reconstruction, defect classification, k-Nearest Neighbors classification, parallel classifier.

1. Introduction

Automatic quality inspection of ferrite cores is a challenging task. In particular, the problem of crack detection can be extremely difficult. While some cracks are quite easy to detect, the others are effectively hidden in the background. Obviously, any system which misses some of the cracks cannot be satisfactory. The current paper considers the case of these hard-to-detect cracks.

A typical ferrite core appears relatively dark in the image. Depending upon the manufacturing process, its surface may be covered by a pattern of traces remaining from the grinding operation carried out on some of the walls of the core. These traces are called grooves and form a pattern of dark and bright stripes that are more or less parallel. The grooves have irregular brightness, variable width, and may be discontinuous. Sometimes the grooves are obviously nonparallel. This happens when the grinding tool rotated with respect to the ferrite core following the circular path of a small diameter. Detection of cracks is particularly difficult in the presence of the grooves, when the cracks have appearance similar to grooves, and even a human expert may need considerable time, positioning herself with respect to the core and the light source, before issuing any conclusive statement. This is a well known problem of low signal-to-noise ratio.

In this paper a two-stage vision system for detection and measurement of crack regions is presented. In the first, detection stage the regions are detected for which there

is a strong evidence that they belong to cracks. The morphological detector used is rather simple, and it detects irregular changes of brightness in the image. Changes corresponding to contours of the cores, for example straight lines or circles, are considered regular and are not detected. The output of the detector is a gray level map of cracks. This map is thresholded so that a binary map of cracks is obtained. Subsequently, a morphological reconstruction of the binary map of cracks is carried out. The resulting reconstructed map usually contains most of the cracks together with the undesired information on grooves, that is some "false alarms." The second stage of the vision system consists of a feature-based parallel k-Nearest Neighbors classifier which analyzes only the pixels belonging to the reconstructed binary map obtained in the first stage. Detector of cracks is fast, but it assigns too many pixels to cracks. The classifier, which is much slower, corrects this result. Crack detection is indispensable for reducing the amount of data sent to the classifier. Experimental results obtained with the developed vision system are presented at the end of the paper. Although the problem of crack detection still awaits its full solution, the authors believe that the experience gathered so far can be useful for other researchers in this field.

2. Lighting

Lighting is vital for the whole process of detection of irregularities. The design criteria for the lighting system were the uniformity and nondirectionality of illumination.

The lighting systems based on fiber optics, light emmitting diodes and microbulbs were tested. In every case light sources were situated on a conical surface rather than on a plane to achieve greater depth of the uniform lightinig. In other words, a nearly flat function of illumination intensity versus radius R and distance H was received for a large range of these parameters (see Fig. 2). The best results in this respect were achieved with the Double Layered LED Illuminator (DLEDI), shown in Figs. 1 and 2. 84 green LEDs of type CQP412 placed in two rows emit together about 1.2 mcd.

The large angle of inclination of the light beam with respect to surface normal makes any deviation from planarity of the tested surface appear as brighter or darker than the surroundings.

3. Detection of cracks

There is a rich literature on mathematical morphology, starting with the early papers [3] and [4]. However, the number of papers related to defect detection is quite limited, probably due to the fact that it is hard to express industrial standards in terms of morphology. Furthermore, there are many forms of defects (and their backgrounds), for which entirely different methods may be needed. Usually the morphologists do not have access to such data and use some accidentally chosen pictures.
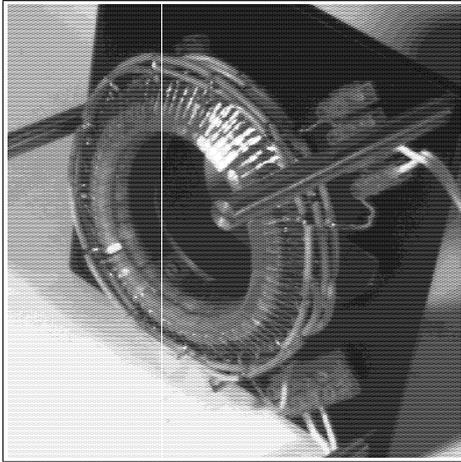
Fig. 1.   The bottom view of the Double Layered LED Illuminator (DLEDI). Two circles of LEDs and wiring are visible.
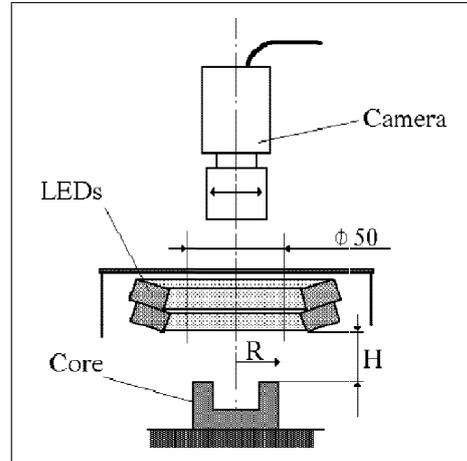
Fig. 2.   The scheme of the DLEDI. The emitting surfaces of the LEDs lie on a conical surface.

The cracks are just one form of defects in ferrites. Other very common defects are chips, pullouts, ragged edges, etc. Sometimes one form of the defect can go over into another, for example a crack can widen and become a chip. This situation suggests that crack detection might be a particular case of (any) defect detection.

A short review of the relevant papers on defect detection includes the following papers. In [8] the use or morphological operations for detection of defects on the matte surface of the TV tube is described. The defects have a form of long, thin, and twisted shapes, whereas noise reveals itself in a form or rounded circular blobs. The analyzed image is binarized, and the skeletons of all shapes are found. Differentiation between defects and noise is based on the analysis of the properties of the skeletons. A sound theoretical approach to defect detection is presented in [11], where structural opening and a top-hat transform are used. Unfortunately, the proposed method is suited mainly to artificially generated textures. In fact, this method is based on "learning the texture," which involves finding the minimal family of structuring elements corresponding to the primitive patterns in the analyzed texture. However, finding such a family for ferrite cores is impossible since the textures on the walls of ferrites do not exhibit sufficient stationarity in a single image and among images of various cores. In [5] a comparison of several variations of improved top-hat transforms is presented. The main advantage of these transforms is a reduced noise sensitivity. The defects described in [5] are located on flat surfaces of metal or wood, and were taken from available objects without consideration of what becomes available on a production line. In [14] the method described in [5]

was developed and adjusted to detection of surface defects of ferrite cores coming from a production line. The main feature of the described defect detector is that it has more or less isotropic properties and detects defects in a very wide range of sizes and shapes. The isotropy of the detector means that no direction in the image plane is privileged, and defects in any direction are detected with the same sensitivity.

The morphological crack detector described in the current paper is a modification of those presented in [14] and [17]. The difference is that the current detector is an anisotropic one, which is more appropriate for the case of crack detection since cracks usually have a form of a long thin and (approximately) straight line segment, or consist of some number of such segments. Furthermore, the anisotropy of the detector allows one to better cope with the pattern of parallel stripes coming from the above mentioned grinding process.

There exist some papers dealing directly with detection of cracks ([16, 18]). The PhD dissertation [18] analyzes images containing lines, both straight and curved. It develops a model in which an image is represented by an unknown number of Bézier curves. The parameters of the model are obtained by reversible jump Markov chain Monte Carlo technique. The main application considered in [16] and [18] is the classification of the craquelure of an old oil painting. Ferrite cores usually do not exibit such nets of cracks as are typical for old paintings. The industrial cracks are more localized and hidden so the discussed method seems not to be suited for the purpose under consideration.

Attempts have been made by the authors to develop an adaptive genetic algorithm based on [15] or an evolutionary system based on [13] for detection of cracks. In [15] the genetic algorihm is used for finding the optimal morphological filter for removing artificially introduced noise into texture images from Brodatz album. The genetic algorithm determines both the sequence of operations and the optimal structuring element. In [13] the evolutionary system is used for optimization of the sequence of operations aiming at recognition of letters. The system was tested mainly on binary images, with possible extension to gray level images. Experience of the authors of the current paper was only partly satisfactory. Although it is possible to employ these innovative techniques, they are complicated and give results which are no better than the results obtained by a simple method described below. It turned out impossible to increase the discriminative power of the defect detector by taking samples of texture corresponding to cracks and crack-free areas and using them for generation of structuring functions which would discriminate between the cracks and grooves from grinding.

An example of the ferrite core with grooves resulting from the grinding is shown in Fig. 3(a). They form a pattern of more or less parallel darker and brighter lines. There is a single bright crack visible in Fig. 3(a) in the upper half of the core. The physical length of the core is 50 mm, and the image shows almost the entire core. The size of the image is 512*128 pixels. The reason for using atypical size of the image is that one wants to have the image filled out with the object as much as possible. Processing "empty"

pixels takes time, and in quality inspection one cannot afford wasting time, particularly when many images are processed.

In order to carry out the described anisotropic morphological operations, the structuring element should be either perpendicular or parallel to the stripes from grinding. The rotation of the ferrite core itself is out of the question since this would be a costly manufacturing operation requiring additional equipment. It would also take a long time. The rotation of small structuring elements, for example of size 5×1, by an arbitrary angle, can only be implemented in a very rough manner since the original pixel in general would not fall entirely into another pixel after rotation and some approximation is necessary. As a result, it turned out more practical to rotate the image of the core. In order to rotate the image, one has first to establish the dominant direction in the image, and then to rotate the image appropriately. The problem of detection of the dominant direction is known from literature ([10]) and will not be entered here. Similarly, the problem of high-accuracy rotation of images using bilinear interpolation of bicubic splines is adequately described in [6]. For the purposes of the described investigation, the images of the ferrite cores were rotated by means of the commercial program, such as the Photoshop. The accuracy of the vertical or horizontal alignment of the stripes in the image is not critical. This is because the structuring elements used are of size, say, 1×5, with 1 denoting the width, and 5 denoting the height of the element. The stripes usually have width of two or more pixels, which means that the vertical stripe will accomodate such element even if this stripe deviates 10 to 20° from the vertical line. Fig. 3(a) shows the image after rotation. In the following only the rotated images are considered.

Detection of horizontal cracks brighter than the surroundings is based on an equation which is an improved version of the top-hat transform ([5, 14])

$$T_h = I - \min[(I \bullet S_h) \circ S_h, I], \tag{1}$$

where I denotes the input image, and T_h is the gray level map of horizontal cracks. I_h is a structuring element for detection of horizontal cracks. The operation symbol in $I \bullet S_h$ (respectively $I \circ S_h$) denotes closing (respectively opening) of the image I by means of the structuring element S_h. In a more general situation, the structuring element S_h would be replaced by an arbitrary element ([14]). It can be shown that due to the closing, opening, and minimum operations, the pixels corresponding to defect-free areas have value 0 (are black) in the map T_h, and pixels belonging to defects (cracks) have some nonzero value, which can be regarded as a "measure of defectiveness." Detection of cracks darker than the surroundings is possible using an equation dual to Eq. (1)

$$T_h = \max[(I \circ S_h) \bullet S_h, I] - I, \tag{2}$$

in which the opening and closing are exchanged, the minimum is replaced by maximum, and the roles of minuend and subtrahend are also exchanged. Due to similarities of analysis, in the following only the cracks brighter than the surroundings are considered.
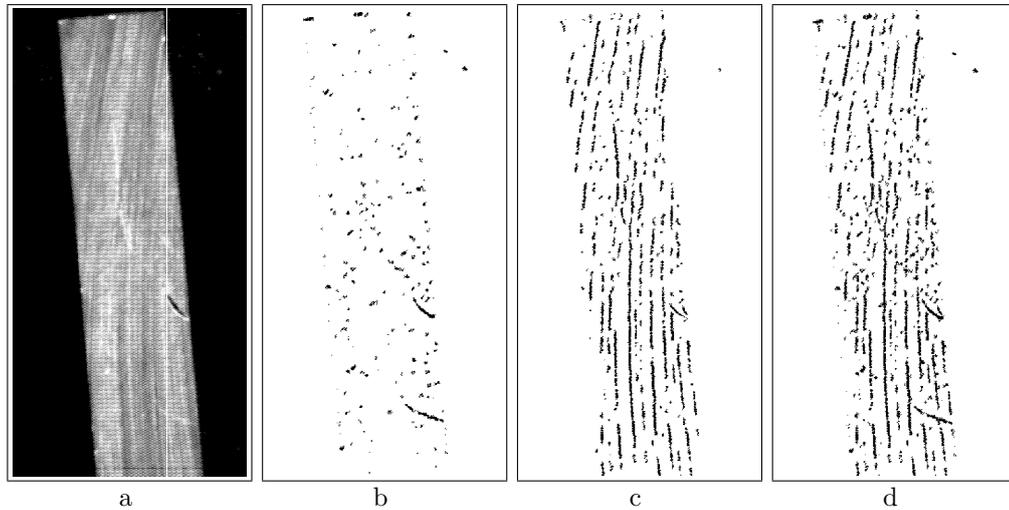
Fig. 3.   Detection of cracks. a) Original image. b) Binary map of horizontal cracks. c) Binary map of vertical cracks. d) Final map of cracks.

For detecting arbitrary, more rounded defects the structuring element of size 3×3 may be used. For detection of horizontal, elongated cracks the *vertical* structuring element of size 1×5 is more appropriate. It was found experimentally that the length of the structuring element is not critical, and for given size of the cores and size of the images the elements of length 3 or 7 might be used as well.

Equation for detecting the vertical cracks is almost the same as Eq. (1)

$$T_v = I - \min[(I \bullet S_v) \circ S_v, I] . \tag{3}$$

The only difference is that for obtaining the gray level map of vertical cracks the structuring element S_v is used, which is in fact a *horizontal* element of size 5×1. Summarizing, in order to detect a crack in a given direction, one has to use the structuring element which straddles across the crack.

The images T_h and T_v are gray level maps, hence not very convenient for consideration. After complementing these maps and thresholding, one obtains the binary maps

$$T_{h5} = \mathrm{TH}_1(\overline{T}_h), \qquad\qquad T_{v5} = \mathrm{TH}_1(\overline{T}_v), \tag{4}$$

in which all pixels having measure of defectiveness below certain threshold have brightness 255 (are white), and all other pixels have brightness 0. This means that cracks are conveniently painted in black on white background. The threshold $\mathrm{TH}_1 = 5$ was chosen experimentally. The main idea was to have a low threshold so that everything which might be suspected of being a crack would be included in the map.

It can be seen in Fig. 1(a) that it is quite hard to distinguish between cracks and brighter stripes from grinding of the ferrites. Thresholding the gray level maps of cracks

with some particular threshold value gives a binary map of cracks which contains masks of both cracks and bright stripes from grinding. In order to improve the binary map of cracks the following approach is used.

The gray level maps are thresholded again, this time however, with a higher threshold $TH_2 = 15$, so that Eq. (4) is replaced by

$$T_{h15} = TH_2(\overline{T}_h), \qquad\qquad T_{v15} = TH_2(\overline{T}_v). \qquad\qquad (5)$$

The idea behind this operation is that cracks are slightly brighter than bright stripes from grinding. As a result one obtains at least some parts of the cracks, and at the same time one gets rid of some stripes from grinding.

The exact shape of cracks is obtained using the binary reconstruction. For details of morphological reconstruction the reader is referred to [7]. At this time suffice it to say that for binary reconstruction two images are used: the mask and the marker. The mask contains a number of blobs, which are known as connected components in the theory of sets. The marker contains another set of connected components. The marker chooses which connected components from the mask should be included in the result of reconstruction. For the appropriate reconstruction the marker should lie under the mask. That means that for each chosen connected component of the mask there should be at least one pixel in the marker, and no pixels of the marker should stick out of the mask. Using the notation introduced in [7] the reconstruction is represented by the equation $I_r = \rho_{\mathrm{mask}}(\mathrm{marker})$. In the case under consideration, two separate reconstructions are carried out for horizontal and vertical cracks, according to the equation

$$I_h = \rho_{T_{h5}}(T_{h15}), \qquad\qquad I_v = \rho_{T_{v5}}(T_{v15}). \qquad\qquad (6)$$

The results of reconstruction of horizontal and vertical cracks are depicted in Figs. 3(b) and (c). The map in Fig. 3(b) is in principle satisfactory. The short pseudomasks representing noise rather than real cracks can be filtered out quite easily. On the contrary, the map in Fig. 3(c) contains masks of cracks together with masks of bright grooves from grinding. Obviously the masks in Fig. 3(c) can not be used in the presented form, and it is necessary to use the classification procedure for removing the masks of the bright stripes. This subject is discussed in detail in the next sections.

By taking the maximum of the complemented maps $\overline{I_h}$ and $\overline{I_v}$, one obtains the complement of the final map $\overline{I_m}$ of cracks

$$\overline{I_m} = \max(\overline{I_h}, \overline{I_v}) \qquad\qquad (7)$$

The map I_m is shown in Fig. 3(d). Slanted cracks which are neither vertical nor horizontal are detected partially by either structuring element. Similarly are detected cracks consisting of several straight line segments.

A detailed example of intermediate results of individual operations for detecting vertical cracks, applied to a selected window of an image from Fig. 3, is shown in Fig. 4.

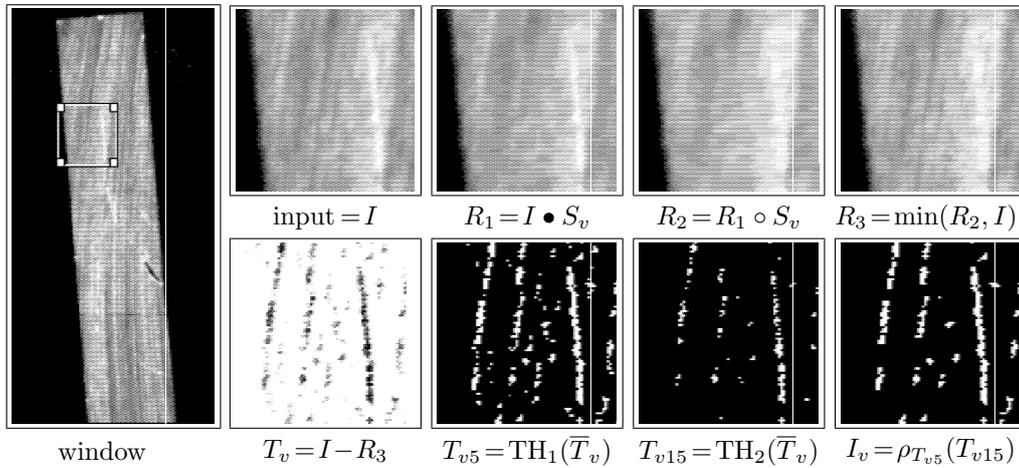|	input $= I$	$R_1 = I \bullet S_v$	$R_2 = R_1 \circ S_v$	$R_3 = \min(R_2, I)$
window	$T_v = I - R_3$	$T_{v5} = \mathrm{TH}_1(\overline{T}_v)$	$T_{v15} = \mathrm{TH}_2(\overline{T}_v)$	$I_v = \rho_{T_{v5}}(T_{v15})$

Fig. 4. Results of individual operations for detecting vertical cracks, applied to a selected window of an image from Fig. 3, described by the Eqs. (3)-(6).

4. Classification

The second stage of the system has a form of a nearest neighbors (NN) classifier ([12]). The principle of a NN classifier is as follows. A set of *reference patterns* with known class assignments called a *reference set* is a basis for classification of an unknown pattern. A *distance function* is defined on the set of patterns. Distances from the unknown pattern to each reference pattern can be calculated, and a set of k nearest neighbors of the unknown pattern can be found. The unknown pattern is assigned to the class to which a majority of these k nearest neighbors belong. The training of a k-NN classifier consists in finding optimal k and forming the reference set. Basically, all the training patterns can enter into the reference set, but this would lead to very inefficient classification.

In the application considered, the classified patterns are pixels. Feature selection and reduction of the reference set is used. Reduction is made primarily to increase the speed of classification; however, it can also decrease the classification error. Here, the parallel net of binary decision k-NN classifiers is used, one for each pair of classes. The final result is obtained by voting carried out between these component classifiers[1]. Each of these classifiers is approximated by a fast 1-NN classifier with the reduced reference set.

For feature selection and selection of the optimal value of k, the *leave-one-out method* ([2]) is used. The condition of *minimum class overlap rate* is used rather than the most frequently used condition of *minimum classification error*. Then, an approximation of

---

[1] In the voting, the classifier for each pair of classes has one vote, and votes for one or the other of the classes it classifies. The class which gathers the largest number of votes wins.

a k-NN classifier by a 1-NN classifier is obtained by reclassification of the reference set with the (k+1)-NN rule. Finally, the reference set is reduced by means of the Hart algorithm ([1]) with modifications ([19]).

4.1. Minimum class overlap rate as the training criterion

It is well known that the objects which are close to the class boundaries in the feature space are more difficult to classify than the ones located far from the boundaries. The number of difficult objects can be used as a feature selection criterion instead of the most frequently used classification error rate.

If nc is the number of classes then the reference set consists of nc subsets $X_i, i = 1, 2, ..., nc$. Each X_i contains only objects from the class i. We associate the sets X_i with the positive real numbers $e_i, i = 1, 2, ..., nc$ defined as follows:

$$e_i = \max_{x_j \in X_i} d(X_i - x_j, x_j), \tag{8}$$

where d denotes a distance function between an object x_j and a set $X_i - x_j$, and x_j is an element of X_i, that is, d is the distance between x_j and the nearest object in $X_i - x_j$. We also define the regions $A_1, A_2, ..., A_{nc}$:

$$A_i = \{x : d(X_i, x) \le e_i\}. \tag{9}$$

Let us denote by A the set of all points in the feature space each of which belongs to only one of the regions $A_i, i = 1, 2, ..., nc$.

Having in mind the above, we can define the *difficult* objects. The object is *difficult* for classification if and only if it falls simultaneously into two or more regions A_i. A ratio obtained by division of the number of difficult objects by the number of objects in the training set will be called the *class overlap rate*. This rate can be easily calculated. For two classes with equal numbers of objects in the training set the class overlap rate requires a twice smaller number of distances to be calculated than those needed for the classical error rate.

The error rate (estimated with the leave-one-out method) for the classifier trained with the minimum class overlap rate as a criterion can be as much as about four times smaller than that for the classical error rate as a criterion ([20]).

4.2. The parallel net of two-decision k-NN classifiers

The k-NN classifier obtained by performing feature selection and finding the optimum k determines nc decision regions in the feature space. Each region corresponds to a different class. The boundary between any two classes i and j depends on the selected features and on the value of k. The selected features as well as the value of k depend on objects from the classes other than i and j. Thus, the objects from the third classes – those different than i and j – influence the shape of the boundary separating the classes i and j. This influence acts as noise.

To reduce the influence of the third classes on the boundary between the two classes i and j, a parallel net of two-decision k-NN classifiers has been recommended ([9]), each of them corresponding to a different pair of classes. Hence, there are $nc(nc-1)/2$ different component classifiers, each for one pair of classes. Feature selection as well as the determination of k are performed for each of the component classifiers separately.

4.3. Approximation with a 1-NN classifier and reduction of the reference set

The use of the k-NN instead of the 1-NN classifier increases the classification quality but makes it slower. To keep the classification speed of the 1-NN classifier and the classification quality close to that offered by the k-NN one, we can approximate the k-NN classifier by the 1-NN one. The only thing we need to do is to reclassify the whole reference set by the $(k+1)$-NN rule, where k is the value found by the leave-one-out method as the one which minimises the error rate. The use of $(k+1)$-NN instead of k-NN results from that this time the classified object belongs simultaneously to the reference set. So, now for each object of the reference set the $(k+1)$ nearest neighbors occupy exactly the same hypersphere as k nearest neighbors during the realisation of the leave-one-out method.

The speed of the 1-NN classifier depends linearly on the reference set size. Hence, the reference set is reduced with the modified Hart's algorithm. The basic rule for reduction is that the results of classification on the training set with the reduced reference set must be the same as those with the full reference set ([1, 19]).

4.4. Training

For calculating the features of a pattern, that is, a pixel, the square and linear neighborhoods of the pixel in the image domain are used, each rotated around its central pixel to make the edges of the neighbourhood normal to the locally dominating direction of texture, defined in [10] in the terms of local spectral analysis of the image. 64 features were experimentally selected from a large set of statistical and textural measures ([17, 19]). It should be mentioned that for none of the pairs of classes the whole set of features was necessary; some were separated with the use of as little as one or two features. However, each of the 64 features was used for at least one classifier.

The training set had 4553 pixels (patterns) obtained by manually pointing pixels in training images. The number of patterns in classes varied from 29 to 1165, depending on how much of the surface of the tested product belonged to the given class. The best represented classes were *edge of the bright groove* and *edge of the dark groove*, and the worse represented ones were related to the class *chip*, as the chips were very scarce in the considered batch of the products. The numbers of training patterns reflected the frequency of occurrence of the respective classes. The strategy for selecting the pixels for training was to choose such pixels for which the classification was clear. It was left to
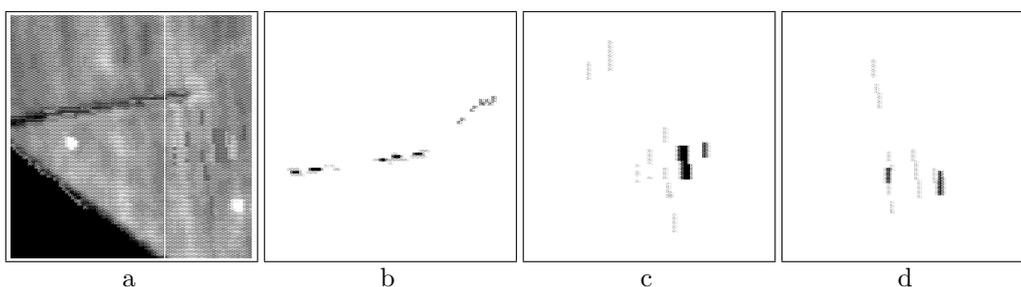
a   b   c   d

Fig. 5. Details of a selected image containing the training patterns (pixels). a) Training image with actually used colours (see text) shown as shades of gray. Two white spots: *good object*; pixels outside the object: *background*. b) Pixels of subclass *dark crack – interior* shown in black, *dark crack – edge* in bright gray, and *bright crack – edge* in dark gray. c) Subclass *dark groove – interior* in black and *dark groove – edge* in gray. d) Same as (c), for subclasses *bright groove*.

the classifier to generalize on these data in order to classify the pixels with less evident class membership.

Names of some of the used 15 classes are self-explaining, like *good surface* and *background*. Other classes correspond to such typical defects of ferrites as a *chip*, *pull-out*, and *crack*, which is the class of main concern in the considered application. The *groove* is another class. Our extensive practice indicates that the classes should be very specific. Therefore, some were subdivided, as for example *bright crack* and *dark crack*, so the total number of classes is large, although actually we need only two general classes: *crack* and *no-crack*, into which the above mentioned classes are merged after classification.

The necessity of such a detailed subdivision of the classes results from the same premises which support the better quality of results of a net of parallel classifiers than those of a single one. The argument of reducing the influence of third classes on training a classifier for a given pair of classes can be repeated here.

An example of a training image is shown in Fig. 5. The technique used was that pixels belonging to each class were marked with a different color: different shades of red – subclasses of the class *crack*, blue – *chip*, shades of violet – *grooves*, etc. In Fig. 5 the colors have been shown as shades of gray.

It should be noted that to prepare the training patterns it is definitely not enough to look only at the images of the tested surface. The original objects, often viewed with the help of a magnifying glass, were observed together with their images.

The results of training can be validated with the use of the classification error estimated on the whole training set. The general error was 1.4%. The reduction of the set of reference patterns together with the feature selection made it possible to attain the classification speed of approximately 230 pixels/s (Pentium 266 MHz, GNU C).
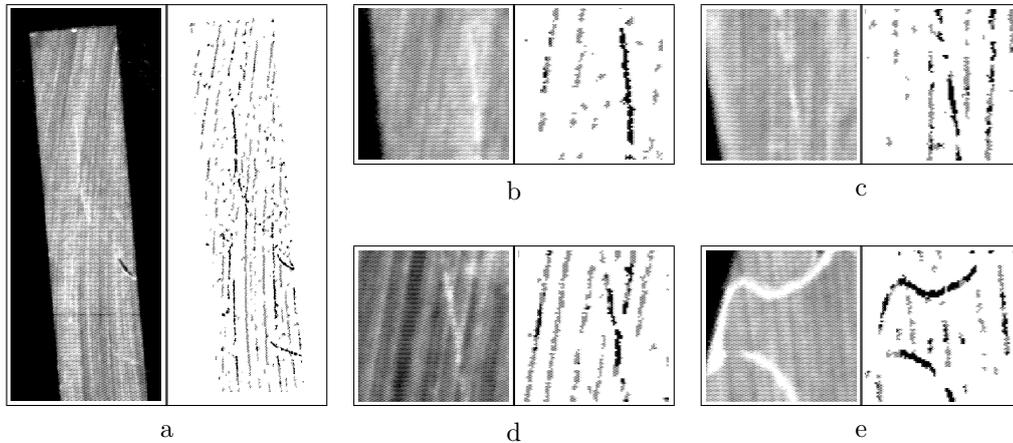
Fig. 6.   Examples of results. Left images in each pair are input images. Right images represent regions found with the morphological detector. Regions assigned to class *crack* in the process of classification are shown in black; regions rejected from the class *crack* are shown in gray. a) Result for image of Fig. 3(a). b) Fragment of (a) magnified. c-e) Results for fragments of other images.

5. Example of results and discussion

Some examples of results received for various images of cracks are shown in Fig. 6. It can be noticed that while a large number of false positive errors made by the morphological detector have been successfully removed by the classifier, some of them still remain. The detector appeared to be excessively sensitive. The likelihood of committing a false negative error by the detector is small.

In the case of image in Fig. 3(a), for which the final results are shown in Fig. 6(a), from about 6600 pixels detected by the detector, 1900 were finally assigned to the class *crack*. From these 1900 pixels about 600 are false positive errors (the few negative errors will be neglected in this simplified analysis). As a result, the error rate of the classifier was 9% (600 errors per 6600 classifed pixels). It is reasonable to relate the errors to the total area of the object, which in this case was 55600 pixels. The detector detected 6600 pixels as *cracks*, from these 1900 correctly. The initial error was then 8.4% ((6600 − 1900) per 55600). After classification, the error was 1.1% (600 per 55600), that is, it decreased 7.8 times.

The number of misclassified pixels (9%) was much larger than it would be expected while considering the estimated error of the classifier (1.4%). This means that in the problem at hand the generalising power of the classifier is small. In other words, the training patterns were not representative enough for the problem. There are two typical reasons for such a situation. First, the number of the training patterns could be too

small. Second, the features used could be not sufficiently meaningful for the problem. In both cases, it is very hard to make any improvement. The training set is huge and the features used were successfully tested in other applications related to the products made from the same or very similar material ([17, 19, 20]). The final conclusion is that probably in the considered problem of detection of cracks in grooved surfaces, the limits of the method have been reached.

It seems that the preferable way of improving the results would be to experiment more with the lighting system to force it to expose cracks more strongly than it is the case with the present lighting.

Detection of cracks using the morphological detector described is carried out in 2-3 seconds, depending on the size of the image and its contents. This time could be made negligible if a hardware morphological processor were used. The classification time for the image in Fig. 6(a) was 30 s (Pentium 233 MHz, GNU C), which is a result located half-way between a laboratory inspection system and an industrial one. Classification of the whole surface of the object present in the image (with the detection phase left out) would be 250 s. This exemplifies the importance of the detection phase to the overall system performance.

6. Conclusion

A two-stage vision system for detection of cracks in ferrite surfaces with traces from grinding has been designed and tested. The morphological crack detector which can operate very fast, particularly if a hardware morphological processor is used, gives results containing a considerable number of false-positive errors. The classification stage reduces the number of these errors to a large extent, but still some grooves remain classified as cracks. The classifier is operating at a considerably smaller pixel rate than the morphological detector, so the detector plays an important role as a data reducing filter.

The whole system is still at a development level. New concepts should be incorporated if an industrially acceptable quality of results is expected. Among various options an improvement of the lighting seems the most viable one.

References

1968
[1] Hart P. E. : The condensed nearest neighbor rule. IEEE Trans. Information Theory, 14(3), 515–516.
1982
[2] Devijver P.A., Kittler J. : Pattern recognition: a statistical approach, Prentice Hall, London.

1986

[3] Serra J. : Introduction to mathematical morphology. Computer Vision, Graphics, Image Processing, 35(3), 283–305.

1987

[4] Haralick B. *et al.* : Image analysis using mathematical morphology. IEEE Trans. Pattern Recognition Machine Intelligence, 9(4), 532–550.

1990

[5] Salembier P. : Comparison of some morphological algorithms based on contrast enhancement – application to automatic defect detection. In: Signal Processing V (EUSIPCO V). Elsevier, 833–836.

1992

[6] Danielsson P. E., Hammerin M. : High accuracy rotation of images. CVGIP Graphical Models Image Processing, 54(4), 340–344.

1993

[7] Vincent L. : Morphological grayscale reconstruction in image analysis: Applications and efficient algorithms. IEEE Trans. Image Processing 2(2), 176–201.

[8] Daut D. G., Zhao D.: A flaw detection method based on morphological image processing. IEEE Trans. Circuit Systems Video Technology, 3(6), 389–398.

1994

[9] Jóźwik A. : Object recognition method based on k nearest neighbors rule. Journal of Communications, 45, 27–29.

1995

[10] Yang G. Z., Burger P., Firmin D. N., Underwood S. R. : Structure adaptive anisotropic filtering for magnetic resonance image enhancement. In: Proc. 6th Int. Conf. CAIP, Springer Verlag, Berlin, 384–391.

1996

[11] Huet F., Mattioli J. : A textural analysis by mathematical morphology. In: Mathematical Morphology and Its Applications to Image and Signal Processing. Eds. P. Maragos *et al.*, Kluwer Academic Publishers, Boston, 297–304.

[12] Jóźwik A., Chmielewski L., Cudny W., Skłodowski M. : A 1-NN preclassifier for fuzzy k-NN rule. In: Proc. ICPR, Vol. IV, track D, IEEE Computer Society, Vienna, 234–238.

[13] Zmuda M. A., Tambourino L. A., Rizki M. M. : An evolutionary learning system for synthesizing complex morphological filters. IEEE Trans. Systems Man Cybernetics, 26(4), 645–653.

1997

[14] Nieniewski M. : Morphological method for detecting defects on the surface of ferrite cores. In: The 10th Scandinavian Conference on Image Processing, Vol. I, 323–330.

[15] Li W., Haese-Coat V., Ronsin J. : Using adaptive genetic algorihms in the design of morphological filters in textural image processing. In: Nonlinear Image Processing, SPIE, vol. 2662, 24–35.

[16] Palmer D. : Splitting images. Cambridge Alumni Magazine, 21–22.

[17] Mari M. *et al.* : The CRASH Project: Defect Detection and Classification in Ferrite Cores. In: Image Analysis and Processing. Ed. A. Del Bimbo. Vol. II, Springer Verlag, Berlin, 781–787.

[18] Varley A. J. : Statistical image analysis method for line detection. PhD dissertation, University of Cambridge, UK.

1998

[19] Jóźwik A., Chmielewski L., Skłodowski M., Cudny W. : A parallel net of (1-NN, k-NN) classifiers for optical inspection of surface defects in ferrites. Machine Graphics & Vision, 7(1/2), 99–112.

1999

[20] Jóźwik A., Chmielewski L., Skłodowski M., Cudny W. : Class overlap rate as a design criterion for parallel Nearest Neighbour classifier. In: Proc. 1st Polish Conference on Computer Pattern Recognition Systems KOSYR '99, Trzebieszowice, Poland, May 24-27.